Scale-up in Turbula mixers based on the principle of similarities

Claire Mayer-Laigle, Cendrine Gatumel, Henri Berthiaux

Scale-up in Turbula® mixers based on the principle of similarities

Claire Mayer-Laigle[a], Cendrine Gatumel[b], and Henri Berthiaux[b]

[a]IATE, Univ Montpellier, CIRAD, INRA, Montpellier SupAgro, Montpellier, France; [b]Université de Toulouse, IMT Mines Albi, UMR CNRS 5302, RAPSODEE, Campus Jarlard, Albi, France

ABSTRACT

Many processes from a wide range of industries use powders as raw materials. In most of them, mixing of dry particles is a critical step. However, the complexity of granular materials leads to difficulties in predicting behavior of powders inside a blender. Cost and amount of raw materials needed to achieve these studies imply that such work is often performed at the laboratory scale. The main challenge then lies in the extrapolation of results from lab to pilot or industrial scale with minimum testing in order to optimize costs. Defining reliable scale-up laws for powder mixers remains one of the main industrial issues. The work presented here concerns the scaling-up of Turbula® mixers that are commonly used both in industry and research. Mixtures obtained in different mixer sizes have been compared on the basis of kinematic and dynamic similarities and discussed according to the different flow regimes involved. The dynamic similarities appear to lead to mixture qualities at different scales closer to each other than those obtained on the basis of kinematic similarities probably because of similar flow regimes. However, some other parameters must be taken into consideration, such as the free surface of powder related to the filling ratio.

KEYWORDS

Turbula® blender; powder mixing; scale-up; kinematic and dynamic similarities

GRAPHICAL ABSTRACT

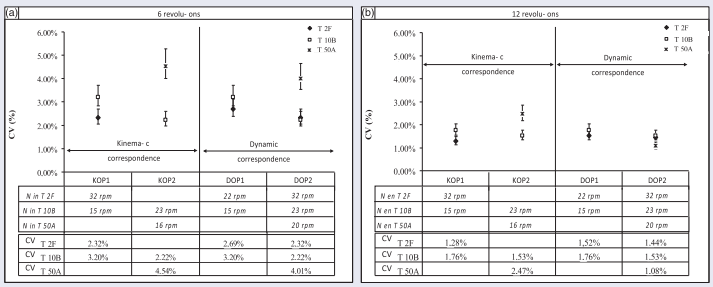

	KOP1	KOP2	DOP1	DOP2
N in T 2F	32 rpm		22 rpm	32 rpm
N in T 10B	15 rpm	23 rpm	15 rpm	23 rpm
N in T 50A		16 rpm		20 rpm
CV T 2F	2.32%		2.69%	2.32%
CV T 10B	3.20%	2.22%	3.20%	2.22%
CV T 50A		4.54%		4.01%

	KOP1	KOP2	DOP1	DOP2
N en T 2F	32 rpm		22 rpm	32 rpm
N en T 10B	15 rpm	23 rpm	15 rpm	23 rpm
N en T 50A		16 rpm		20 rpm
CV T 2F	1.28%		1.52%	1.44%
CV T 10B	1.76%	1.53%	1.76%	1.53%
CV T 50A		2.47%		1.08%

Variation coefficients obtained for the operating points KOP1, KOP2, DOP1 and DOP2 at 6 (a) and 12 (b) revolutions for a cohesive blend.

HIGHLIGHTS

- We define scale-up laws for powder Turbula® blenders from lab to industrial scale.
- Kinematic and dynamic similarities were studied for three sizes of mixer.
- Dynamic similarities lead to similar mixture qualities at different scales.
- Kinematic and dynamic similarities are discussed according to powder flow regimes.

1. Introduction

Granular materials are present in numerous processes, in all industrial sectors. In many of them, mixing or premixing of dry particles is a critical step since it controls the properties of the finished product (color, taste, bioavailability of a drug) (Shenoy et al. 2015). It can influence the downstream steps (Zhou and Morton 2012), as for example, in dry lubrication processes (Suzuki et al. 2015). At the process scale, granular materials can be seen as a state of matter at the crossroad between the solid and the liquid states (Redaelli et al. 2017). Granular materials appear as a multitude of grains, behaving as a solid in isolated form and exhibiting internal discontinuities, according to the size, the shape, and the nature of the interactions (Shah et al. 2017). These discontinuities induce a partial transmission of the stresses during the process, making the behavior of the raw material

CONTACT Cendrine Gatumel Cendrine.gatumel@mines-albi.fr Université de Toulouse, IMT Mines Albi, UMR CNRS 5302, RAPSODEE, Campus Jarlard, F-81013, Albi, France.

difficult to describe, flowing sometimes as a liquid or aggregating under the form of clusters (Savage 1984).

These complex systems cannot be easily described through a limited number of physical parameters (Ammarcha et al. 2013). Simulation could be used to understand mixing mechanisms inside the blender in order to improve design or operations (Yamamoto, Ishihara, and Kano 2016) (Qi, Heindel, and Wright 2017) (Xiao et al. 2017), but this data is difficult to transpose to a real material, for which shapes and sizes of particles are widely dispersed. Therefore, the optimization of mixing or a formulation step cannot be performed without experimental work that is usually tedious. The cost and the quantity of raw materials needed to achieve these studies imply that such work is often performed at the laboratory scale. The main challenge lies then in the extrapolation of results from lab to pilot or industrial scale through a small number of tests. The invariant involved in scale-up strategies of the mixer is generally a quality index but some other values are sometimes considered, such as for example, a velocity of displacement of particles in the case of fragile or friable products (Suzuki et al. 2015). The extrapolation work is never simple since the methods typically used in chemical engineering are not really adapted to granular materials (Bridgwater 2012). The scale-up of powder mixers is still poorly studied in the scientific literature, most of the work has focused on the understanding of mixing mechanisms, which is often a prerequisite to the scale-up.

Nevertheless, over the last 5 years, several publications explored scale effects of granular mixing (Marmur and Heindel 2017) and the scale-up of some common dry powder mixers based on different strategies: a detailed description of the mixing operation based on mathematical equations for rotary drums (Ding et al. 2001), the principle of similarities for rotating drum (Alexander, Shinbrot, and Muzzio 2002), the use of numerical simulation for continuous rotary blade mixers (Yijie, Muzzio, and Ierapetritou 2013), the use of some dimensionless numbers such as the Froude number for a high shear mixer (Cavinato et al. 2013), the construction of an empirical model for V-blenders (Suzuki et al. 2015) and the Power Number for a rotor-stator mixer (James et al. 2017).

The difficulty to obtain homogeneous powder mixtures guaranteeing the quality criteria has led to the development of a wide range of mixers using inertia or G-force to overcome the particular interactions and favor the intimate mixing of all constituents. To prevent segregation phenomena, mixers generating a non-regular motion are often preferred. However, in this case, scale-up rules are even more difficult to define, as the motion of particles is complex. The Turbula® mixer is commonly used for the homogenization of many powder systems in both industry and research (Kushner 2012). Its efficiency is mainly based on the combination of three motions, namely, a revolution, a translation, and an inversion (Wohlhart 1981). This results in a three-dimensional and nearly chaotic motion that helps in obtaining a homogeneous mixture rapidly for many granular systems. The motion of the mixer and mixing dynamics for

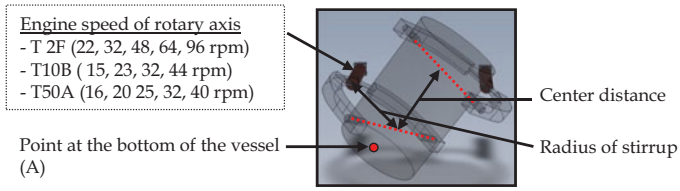

Figure 1. Schematic representation of a Turbula mixer.

an easy flowing powder blend has been described in a previous paper (Mayer-Laigle, Gatumel, and Berthiaux 2015). Cascading regime has been found to be the best one for homogenization. In the present work, we explore the potential of geometric, kinematic, and dynamic criteria, as well as flowing regimes to define scale-up rules for Turbula® mixers with the aim of reaching the same mixture quality for both easy-flowing and cohesive powder blends.

2. Materials and experimental procedures

2.1. The Turbula® mixer

In the Turbula® mixer, the powders to mix are poured into a closed container which is inserted in a mixing basket set by 2 stirrups at 2 rotary axes (see Figure 1). One of them drives the whole system by rotating at a fixed speed, henceforth called engine speed, which can be adjusted. The movement of the system is possible if and only if the radius of the stirrup is equal to the center distance between the two stirrups (Wohlhart 1981). The mixing basket can hold any form of container, henceforth called vessel, fixed thanks to elastic bands.

The three Turbula® scales available on the market were investigated in this work, namely, laboratory Scale – Turbula® T 2 F (2 l), pilot scale – Turbula® T 10B (17 l), industrial scale – Turbula® T 50 A (50 l). The latter corresponds to the maximum size of the standard vessel provided for the equipment. The motion of the vessel is driven by the speed of the rotary axis. Four or five speeds are available according to the different device's scale and are summarised in Figure 1.

2.2. Raw powders flow properties and composition of the different blends

The behavior of powders inside the vessel depends both on process parameters and flow properties of powders. To give a more complete view of scaling parameters inside the mixer, two powder blends of different flow properties have been studied. Each blend is composed of two constituents in relative proportion by weight 85:15. The first blend, qualified as a free flowing blend (FFB), is made of lactose GRANULAC 140 (85% *w/w*) marketed by the company MEGGLE and commercial couscous of durum semolina (15% *w/w*). Couscous particles have been dyed black by iodine adsorption to increase the color contrast between the two constituents for further image analysis (procedure detailed later). The second blend, called composite cohesive blend (CCB), is made up of 85% graphite (Timrex KS 150

Table 1. Powder characteristics and composition of the different blends.

	Free flowing blend		Composite cohesive blend	
	Lactose	Couscous	Graphite	Polymeric matrix
Relative proportion by weight	85%	15%	85%	15%
D_{50} (μm)	59	979	57	121
DI	1.95	0.72	2.66	3.40
I_{carr}	38%	7.3%	25%	42%
R_H	1.61	1.08	1.34	1.73
Flowability	Very bad	Very good	Bad	Execrable
Compressibility	High	Low	Medium	High

Table 2. Calculated mass of the components for the make-up of the different powder blends at the three scales.

	Turbula® T2F	Turbula® T10B	Turbula® T50A
Volume of the container	2 L	17 L	55 L
Mass of the blend	420 g	3570 g	11550 g
Mass of major component (lactose or graphite)	357.0 g	3034.5 g	9817.5 g
Mass of minor component (polymeric matrix or couscous)	63 g	535.5 g	1732.5 g

by society TIMCAL) and 15% thermossetting polymeric matrix (with 97% epoxy resin DGEBA produced by the company RAIGI). This blend, as opposed to the first one, has an industrial purpose as it is intended for the manufacturing of bipolar plates for fuel cells. The volumetric median particle size and the dispersion index, $DI = \frac{(d_{90}-d_{10})}{d_{50}}$, which characterizes the particle size span, have been determined for each powder by LASER diffraction using a Malvern Metasizer Scirocco 2000 (Malvern Instruments Ltd., United Kingdom) and are reported in Table 1. In the case of the composite cohesive blend, the properties of the termossetting polymeric matrix have been approximated by those of the epoxy resin.

To estimate the flowability of each powder, Carr index and Hausner ratio have been determined from the bulk (ρ_a) and bulk packed densities (ρ_p, after 500 taps) measured thanks to a volumenometer Erweka SVM 22, and according to Equations (1) and (2). From these values, appreciations of the compressibility and the flowability of each powder have been given according to Carr (Carr 1970) and Hausner (Hausner 1967). These results are summarized in Table 1.

$$I_{Carr} = \frac{\rho_p - \rho_a}{\rho_p} \quad (1)$$

$$R_H = \frac{\rho_p}{\rho_a} \quad (2)$$

Couscous exhibits a very small Carr Index and Hausner ratio and can be considered as a free-flowing powder. In contrast, Lactose shows very bad flowability. The flowability of the FFB is expected to be intermediate between that of each powder (Demeyre 2007). Indeed, the blend Carr Index is 24.47% demonstrating an easy flowing behavior. Thus, the strong difference between the particle sizes of lactose and couscous is expected to induce a segregation phenomenon during the mixing. For the CCB, the flowability and the median diameter of each powder are closer. The flowability of the mixture is expected to be similar to those of the powders and could be qualified of cohesive with no trend to segregation.

2.3. Powder blending protocol

The powders have been mixed in stainless steel vessels (2 L for T2F, 17 L for T 10B, and 55 L for the T 50 A) with a volumic filling ratio of approximately 50%. The powders were weighed directly in the mixing vessel to prevent possible powder losses during handling. The mass of each constituent for all Turbula® scales is summarized in Table 2. After choosing the engine speed, the mixing operation has been started for a pre-defined number of revolutions.

2.4. Assessment of blend's homogeneity

The quantitative characterization of mixture quality requires the prior set-up of a sampling procedure (number and size of samples, "how to withdraw them?"), as well as the use of a reliable method of measurement of the sample's composition. The method of measurement has to be adapted to the nature of the powders as well as to the intended use of the final product. In this work, a method has been developed for each blend.

Mixture homogeneity is commonly assessed by the coefficient of variation of the key component's compositions in the samples (i.e. lactose in FFB and graphite in CCB). A small CV means that the sample compositions are close to each other and reflects a high homogeneity of the mixture:

$$CV = \frac{\sigma}{\mu} \quad (3)$$

with μ = average composition in key component of the samples analyzed and σ = the standard deviation associated.

2.4.1. Sampling procedure and composition measurement for the free flowing blend

After mixing, the FFB is discharged through a funnel onto a conveyor belt (Massol-Chaudeur, Berthiaux, and Dodds 2002). An inclined piece of stiff cardboard allows the formation of a thin powder layer of constant width and thickness (see Figure 2(a)). There is no high fall of powder in our device, which is known to be one of the main causes of segregation. Vibrations do not occur over a long distance. The cardboard piece displays the powder on the conveyor and

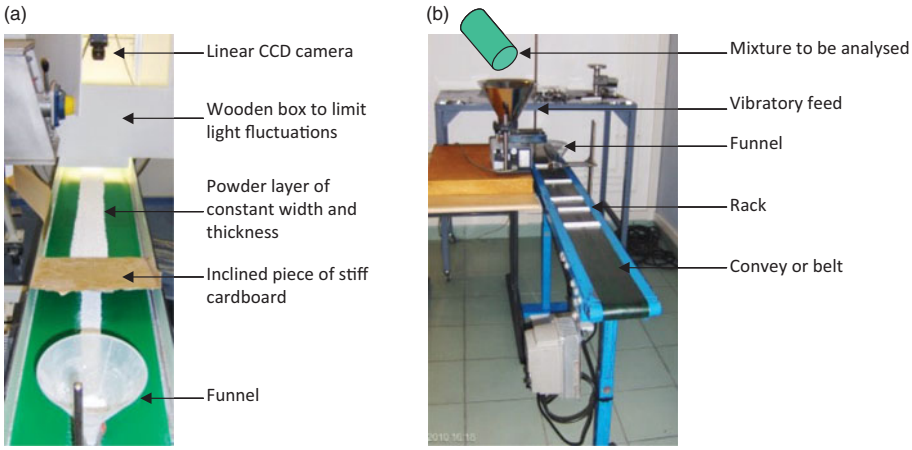

Figure 2. Device for analyzing the composition of the free flowing blend (a) and sampling procedure for the composite cohesive blend (b).

may also induce local segregation, which is the same for all experiments we compare.

The color difference between the lactose (white powder) and the couscous (colored in black by iodine adsorption) allows assessment of the powder homogeneity by an image processing technique according to the protocol developed by Mayer-Laigle, Gatumel, and Berthiaux (2015). The measurement chain consists of a linear CCD camera placed over the conveyor belt and a computer. A time sequence of images is captured and treated with a program developed on the Labview software to determine its composition. Each image acquired corresponds to an independent sample of approximately 0.6 g. Blend homogeneity is assumed to be even when observed on the surface and inside the volume of the powder layer. By this way, the whole blend is fictitiously split into samples and analyzed, therefore, homogeneity can be obtained without any statistical assessment.

2.4.2. Sampling procedure and composition measurement method of the composite cohesive blends

The powder is discharged via a vibratory feeder onto a conveyor belt whose speed is adjustable. In accordance with the industrial final use for this blend (bipolar plate for fuel cell), the scale of scrutiny was evaluated to 70 mg. No online measurement was easily implementable and an exhaustive sampling procedure was not an option as the number of potential samples is 6000, 51,000, and 165,000 for the T2F, T10B, and T50A, respectively. Eighty samples are withdrawn randomly, thanks to racks laid on the conveyor belt (see Figure 2). The mass of the sample has been set to 70 mg by adjusting the speed of the conveyor and the amplitude of vibration. The determination of the composition of each sample is based on the combustion of the thermosetting polymer in an oven at 550 °C for 2 hours. TGA confirmed that the polymer is completely burned without any residual ash. A weight loss of 0.4% was also observed for the graphite because of some moisture adsorbed on the surface of graphite particles. Composition of graphite inside the sample is determined as the ratio between the corrected mass of graphite (to account for the weight loss of 0.4%) and the sample mass. To represent standard deviation results on diagrams, a 90% range of confidence will be drawn according to a χ^2 law. Mixture homogeneities are compared according to this statistical analysis.

3. Principe of similarities in the Turbula® mixer

In basic chemical engineering, two systems at different scales are considered as completely similar if they take place in a similar geometrical space and if all the dimensionless numbers used to characterize the process are equal (Langhaar 1980). In practice, it is impossible to reach a complete similarity, especially with granular materials for which a classical dimensional analysis is arduous to conduct (Ding et al. 2001). In the following, the principle of similarity is applied in a simplified way based on both geometric and kinematic or dynamic similarities. Results obtained with kinematic based similarity and dynamic based similarity will be discussed in order to determine which phenomenon is preponderant to obtain homogeneous mixtures (flowing velocity, centrifugal force, etc).

3.1. Geometrical similarities

Two systems are geometrically similar if they exhibit a constant ratio between all their dimensions. In practice, even if suppliers try to abide by the geometric similarities, there are always some distortions (Cavinato et al. 2013) due to the mechanical environment (constraint) or simply due to the roughness of the surface that cannot be extrapolated (Midoux 1985).

In the Turbula® mixer, the dimensions that influence the motion of the powder are the diameter and length of the vessel, as well as the radius of the stirrup. These characteristic dimensions are summarized in Table 3 for the three scales. The ratios of the characteristic lengths of T10B and T50A on those of T2F were calculated. They are almost identical for all characteristic lengths (≈1.8 for T10B and ≈2.8 for T50A). A slight distortion on the diameter of the vessel does exist for the pilot scale mixer (T10B), but we assume that globally, the different scales appear to comply with geometric similarities.

Table 3. Characteristic dimensions for the Turbula® T2F, T10B et T50A.

	Laboratory scale: T2F	Pilot scale: T10B		Industrial scale: T50A	
			$\frac{d_{T10B}}{d_{T2F}}$		$\frac{d_{T50A}}{d_{T2F}}$
Volume of the container	2 L	17 L	8.5	55 L	27.5
Radius of the stirrup	130 mm	225 mm	1.73	360 mm	2.77
Diameter of the vessel	130 mm	252 mm	1.93	370 mm	2.84
Length of the vessel	200 mm	360 mm	1.8	565 mm	2.83

3.2. Kinematic and dynamic similarities

Kinematic similarities between the two scales imply that two corresponding points will undergo a similar trajectory within a similar time. In the case of a liquid, this means that the fluid streamlines are the same. For a powder, streamlines are not clearly defined and the motion of particles inside a mixer is difficult to predict. Dynamic similarities refer to a same ratio between forces acting on corresponding points in each system. In general, for powder mixing, authors assume that kinematic similarities are satisfied if particles have the same velocity at each mixer scale (Alexander, Shinbrot, and Muzzio 2002), (Nakamura et al. 2009). Concerning dynamic similarities, they are respected when the ratio of forces acting on corresponding points in each system is kept equal. In case of powder, the mixture is achieved most of the time, thanks to the combination of inertial and G-force and the holding of dynamic similarities is often translated to a constant Froude number between the scales. However, if the use of the Froude number is widespread to extrapolate blenders, it has not been proven that it is the only criteria to be taken into account (Landin et al. 1996), (Ding et al. 2001), (Cleary and Sinnott 2008). For example, energetic or kinetic criteria may also be considered

The motion of the Turbula® mixer is complex, nearly chaotic. The particles inside the vessel are submitted to forces and velocities of widely variable directions and amplitudes, according to their positions in the powder bed and to the process parameters (input speed of the rotary axis, size of the mixer, …). In a previous work (Mayer-Laigle, Gatumel, and Berthiaux 2015), the three mixers have been modeled with Solidworks® software in order to thoroughly study the motion of the vessel. In particular, we show that it can be decomposed in displacement, rotation, and reversal phase. We also show that a point at the bottom of the vessel (Point A, in Figure 1) could be used to broadly describe the motion of the powder bed. This point corresponds to the bottom of the powder bed in the initial configuration. During the rotation, the powder is "reversed" and then the velocity and the acceleration at point A can be seen as the initial falling conditions of the particles from the top to the bottom of the vessel. Indeed, mixing is supposed to happen in flows during falling situations, as in a rotating drum. We assume that all the particles in the powder bed will be near this point at a given time and will be submitted to similar forces and velocities.

During a period of rotation, the kinetic profile of the point A shows a maximum which corresponds to displacement phases of the vessel and we define kinematic criteria based on the maximum velocity at this point. (see Figure 3).

For dynamic similarities, the main forces that act on the powder during the mixing process are, respectively, the G-force and the centrifugal force. The Froude number, which is defined as the ratio of the inertial force on gravity, at the reference point has been chosen as the dynamic criteria (Equation 4).

$$\mathrm{Fr} = \frac{\text{Inertial Force}}{\text{Gravity force}} = \frac{a}{g} \tag{4}$$

In the above, g is the acceleration due to gravity (9.81 $m.s^{-2}$) and a is the acceleration for the reference point A at the bottom of the vessel. As can be seen on Figure 3, the acceleration profile of this point also shows a maximum corresponding to reversal phases of the vessel. Maximal Froude numbers for the reference point have been extracted from the simulations and have been chosen as a dynamic criterion.

The evolution of the maximal velocity and the Froude number as a function of the engine speed are shown in Figures 3(a,b), respectively for the different scales. The dots correspond to the Solidworks® calculated values and linear regressions are featured on the graph.

For each scale, the maximum velocity is proportional to the engine speed *N*. Similarily, Froude numbers are proportionnal to N^2. One can note that the ratio between the slopes of linear regressions for the different Turbula scales is similar to those between the characteristic lengths (see Table 3):

$$\frac{a_{T50A}}{a_{T2F}} \approx \frac{b_{T50A}}{b_{T2F}} \approx 2.8 \text{ and } \frac{a_{T10B}}{a_{T2F}} \approx \frac{b_{T10B}}{b_{T2F}} \approx 1.8 \tag{5}$$

with a_{T2F}, a_{T10B}, $a_{T50A,}$ *and* b_{T2F}, b_{T10B}, b_{T50A}, the slopes obtained for the T2F, T10B, and T50A for the maximum velocity and the Froude number, respectively.

Indeed, in the Turbula® mixer, the only parameters that could influence the velocities and accelerations are the characteristic lengths of the mixer and the engine speed. In the different mixers, the velocity varies from 0.5 $m.s^{-1}$ to almost 2.5 $m.s^{-1}$. The velocity obtained in the T50A for the input speed of 40 rpm cannot be reached in the T2F or the T10B. For example, a similar velocity ($V = 0.4$ $m.s^{-1}$) at the bottom of the mixers is obtained when using an input speed of either 8 rpm in the T2F, about 12 rpm in the T10B, or 22 rpm in the T50A. Similarly, the maximum Froude number ($Fr = 4.5$) can only be reached in the T2F for the input speed of 96 rpm and is more than twice the maximum Froude number obtained in T10B ($Fr = 1.7$ for an input speed of 44 rpm) and T50A ($Fr = 2.2$ for input speed of 40 rpm). A similar Froude number of 0.5 can be obtained in

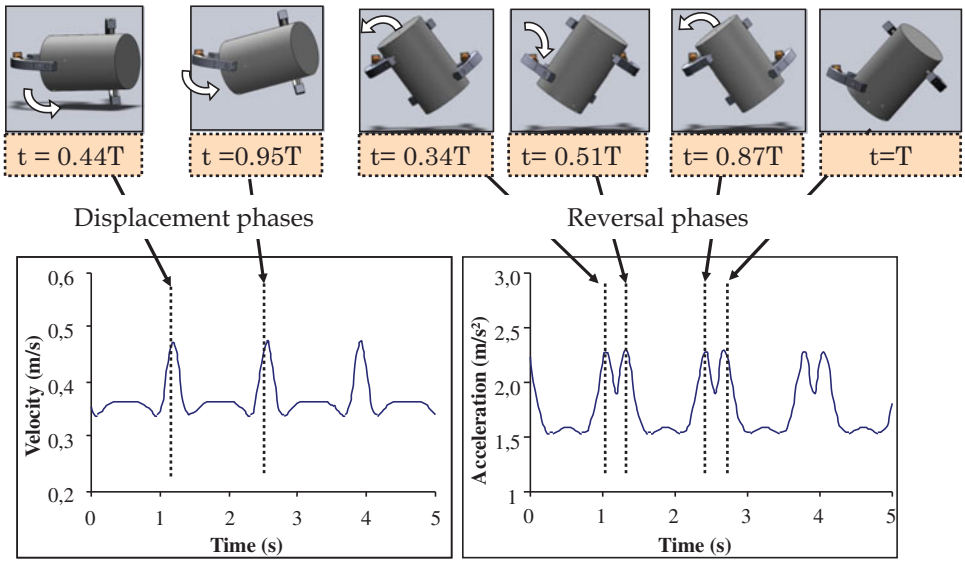

Figure 3. Kinetic and acceleration profiles over a period of time for point A in T2F–22 rpm. The position of the vessel extracted from the simulation have been displayed in the figure. The white arrows indicate the direction of the motion.

Table 4. Kinematic operating points (KOP) for each scale of Turbula® mixers.

	N in T2F	N in T10B	N in T50A	Maximum velocity in point A, $m.s^{-1}$
KOP1	32 rpm	15 rpm		≈0.6
KOP2	46 rpm	23 rpm	16 rpm	≈1.0
KOP3	67 rpm	32 rpm	20 rpm	≈1.2
KOP4		44 rpm	25 rpm	≈1.6
KOP5	96 rpm		32 rpm	≈2.0

Table 5. Dynamic operating points (DOP) for each scale of mixer.

	N in T2F	N in T10B	N in T50A	Maximum Froude number in point A
DOP1	22 rpm	15 rpm		≈0.2
DOP2	32 rpm	23 rpm	20 rpm	≈0.5
DOP3	46 rpm	32 rpm	25 rpm	≈0.9
DOP4	67 rpm	44 rpm	40 rpm	≈2

the T2F, T10B, and T50A for input speeds of 32, 24, and 20 rpm, respectively. However, for each mixer scale, there are only 4 or 5 engine speeds available (actual engine speed) and it is not possible to obtain exactly the same velocity or Froude number in different scales. To overcome this and enable comparisons over the scales, Kinematic (KOP) and Dynamic Operating Points (DOP) have been defined (Tables 4 and 5) in such a way that the relative differences between the equivalent engine speeds (determined from the linear regression on Figure 4) and the actual engine speed are as low as possible and always less than 15%. For most kinematic operating points, the comparison will only involve two sizes of mixers. Only the KOP2 and KOP3 allow a comparison between the three scales.

The velocity and acceleration profiles in point A have been compared for the different operating points and Figure 5 shows those obtained for the KOP2 (Figures 5(a,b)) and DOP3 (Figures 5(b,d)), respectively. The dimensionless time (τ) was obtained by dividing the time by the motion period, i.e. the duration of one rotation of the engine axis. Good adequacy of velocity profiles at the three blender sizes is observed in case of kinematic similarities (Figure 5(a)) and the same goes for accelerations in the case of dynamic similarities (Figure 5(d)). However, as can be seen in Figures 4(a,b) for kinematic as well as 5c and 5d for dynamic similarities, both criteria cannot be met simultaneously.

3.3. Flow regimes in the different Turbula® scales

Several studies, in particular, on rotating drums, have shown that the state of the mixture is mainly related to the flow regime that takes place inside the mixer (Henein, Brimacombe, and Watkinson 1983; Mellmann 2001; Yang et al. 2008), as defined on the basis of the Froude number and the filling degree of the blender. According to the flow regimes, the mixing mechanisms may differ and drive to different mixture patterns (Mayer-Laigle, Gatumel, and Berthiaux 2015). Drawing upon these studies, three flowing regimes in the three Turbula® scales for the different engine speeds have been defined (see Table 6):

i. A cascading regime when Fr $\leq$0.5. In this case, G-force mainly governs powder flow in the mixer and the flow regime is quite similar to the cascading regime in a rotating drum.
ii. A cataracting regime for Froude numbers between 0.8 and 2.5, where both gravity force and centrifugal force are responsible for the state of the mixture.
iii. A collisional regime for which the centrifugal forces are predominant and mixing is probably achieved, thanks to diffusion (Fr $\geq$ 2.5). It can be noted that the collisional mode is only possible in the T2F.

Experimental results obtained in the different scales can now be compared on the basis of the different kinematic and dynamic operating points, keeping in mind the different flow regimes inside the mixers.

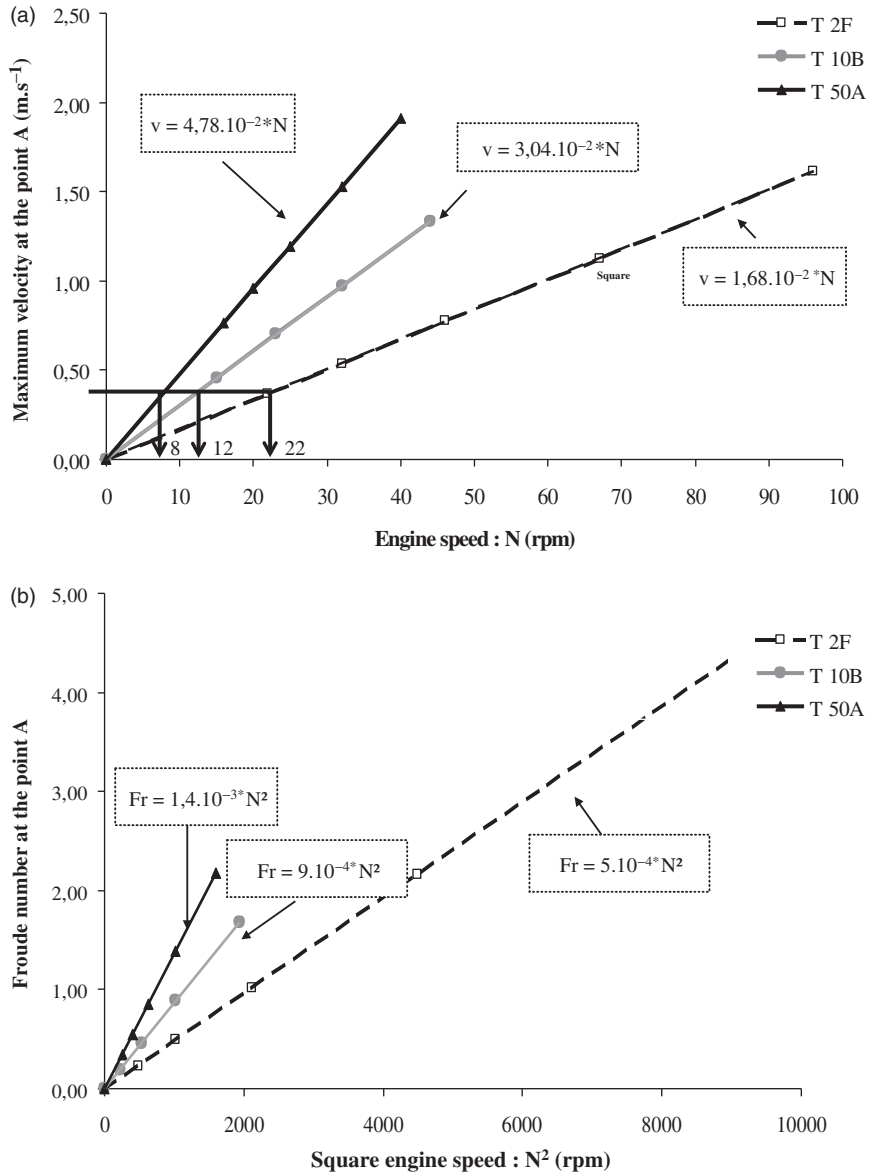

Figure 4. Maximum velocity (a) and Froude number (b) for the different Turbula® scales, calculated values (dots) and linear regressions.

4. Experimental comparison of powder homogeneity at the three mixer scales based on kinematic or dynamic criteria

The challenge when scaling up a powder mixer is to keep the same mixture quality whatever the size of the mixer. In this study, for each blend, we compare the coefficients of variation CV obtained after a definite time in the three different scales for the same kinematic and dynamic operating points. To achieve a reliable comparison between the different scales, mixtures have been compared on the basis of the same number of revolutions.

4.1. Scaling-up the free-flowing blend

A previous study in T2F has shown that homogeneity of FFB achieved after a small number of revolutions may vary widely because of various segregation effects involved in the different flow regimes (segregation by rolling when Fr > 0.5, by trajectory when $0.5 < Fr < 2.5$ and by percolation when Fr = 4.5). It has been demonstrated that 500 revolutions allow to reach a stable mixture, whatever the rotational speed is and then, the CV obtained depend on the engine speed N (Mayer-Laigle, Gatumel, and Berthiaux 2015). The homogeneities of the free-flowing blend obtained in T2F and T10B have been compared for 500 revolutions at the KOP1, KOP2, KOP3, DOP1, DOP2, DOP3, and DOP4. Due to experimental constraints, experiments in T50A have not been realized. The results obtained are presented in Figure 6. For each operating point, the corresponding engine speeds and value of CV have been noted on the figure. A relative discrepancy between the two values of CV has been calculated according to Equation (6).

$$\text{Discrepancy} = \frac{|CV_{T2F} - CV_{T10B}|}{{}^{1}/_{2} * (CV_{T2F} + CV_{T10B})} \tag{6}$$

with CV_{T2F} and CV_{T10B} being the values of CV obtained in T2F and T10B, respectively.

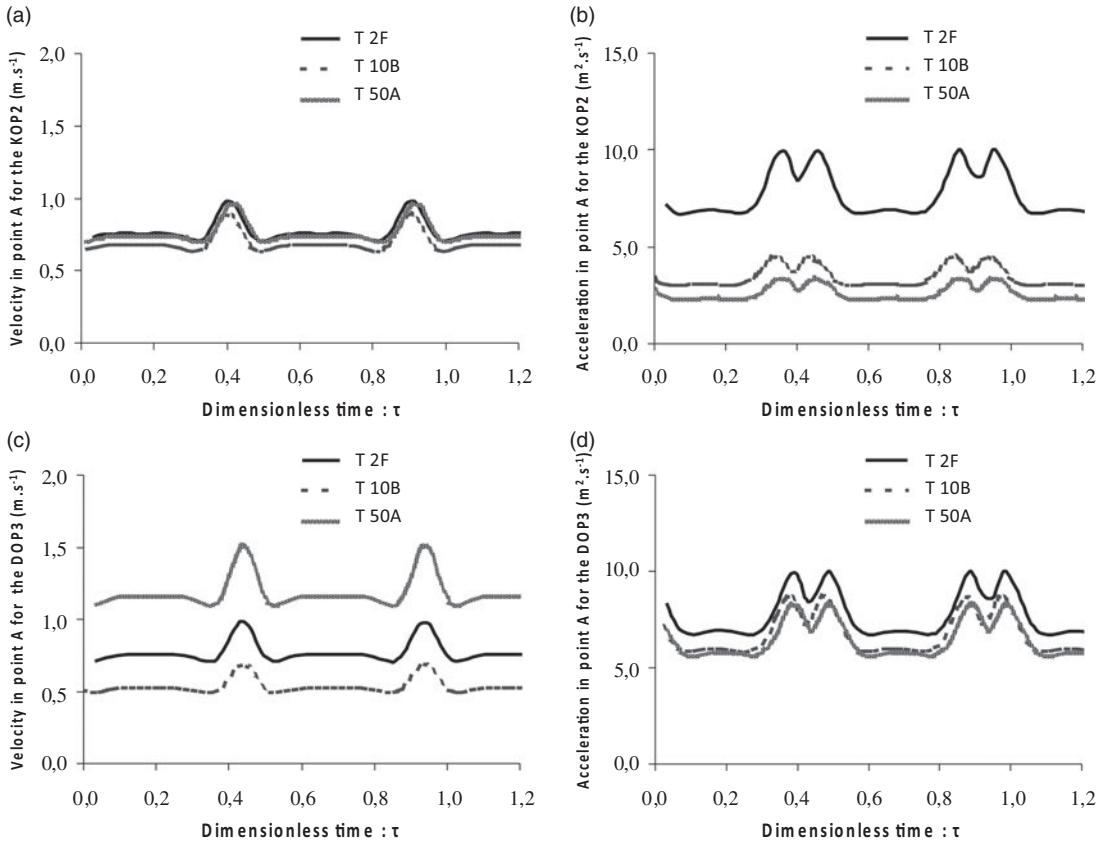

Figure 5. Velocity and acceleration profiles at the kinematics operating points 2 (a and b) and at the dynamic operating points 3 (c and d) as a function of the dimensionless time (time divided by the period or rotation of the tank T).

Table 6. Flow regimes for the different engine speeds according to the determination of the Froude number [Mayer-Laigle, Gatumel, and Berthiaux 2015].

	T2F		T10B		T 50A	
Flow regimes	Engine speed	Fr	Engine speed	Fr	Engine speed	Fr
Cascading	22 rpm	0.2	15 rpm	0.2	16 rpm	0.3
	32 rpm	0.5	23 rpm	0.5	20 rpm	0.5
Cataracting	46 rpm	1.0	32 rpm	0.9	25 rpm	0.8
			44 rpm	1.7	32 rpm	1.4
	67	2.2			40 rpm	2.2
Collisional mode	96	4.5				

For the KOP1 and KOP3, we can observe a small discrepancy between the values of the CV obtained (≈5%). In contrast, the discrepancy for the KOP2 is 17.9% (Figure 6(a)). The kinematic criterion, therefore, leads to a high difference in term of mixture homogeneity according to the engine speeds considered and does not seem to be robust for scaling-up Turbula® mixers for an easy flowing powder. Considering the dynamic criterion (Figure 6(b)), the discrepancy between the value of CV are on average lower and always below 8.5%. This criterion seems to be more adapted to predict mixture quality. We can also note that the evolution of the CV with the rotational speed is identical in both scales, with an increase between the DOP2 and DOP3.

However, for all experiments realized at an equivalent engine speed, the CV obtained in the T10B are always smaller than those obtained in the T2F, reflecting in a higher homogeneity for the mixtures at this scale.

The engine speeds in T2F and T10B for the KOP1 correspond both to a cascading flow regime. Similarly, for the KOP3, the powder blends in both scales are in a cataracting flow regime. On the contrary, at the KOP2, the engine speed of 46 rpm in T2F corresponds to a cataracting regime and the engine speed of 23 rpm in T10B to a cascading regime. This difference of flow regime could explain the significant gap observed between the CV in T2F and T10B for the KOP2. Likewise, the increase observed between the DOP2 and DOP3 can be related to the transition between the cascading and cataracting modes in both scales. Indeed, the free-flowing blend tends to segregate and the cataracting regime increases this phenomena.

In addition, in each scale, the values of the CV obtained for the cascading mode are nearly equal: (i) 2.23 and 2.16% in T2F for 22 and 32 rpm, (ii) 2.04 and 2.05% for 15 and 23 rpm in T10B. The same applies for the cataracting mode in which the values of the CV measured are very close (2.43 and 2.46% in T2F for the engine speed 46 and 67 rpm and 2.40 and 2.32% in T10B for the engine speed 32 and 44 rpm). These observations suggest that in the case of an easy flowing powder, the mixture homogeneity obtained is more related to the mixing mechanisms depending on the flow regimes rather than to the velocity of the particles inside the mixer.

4.2. Scaling-up the composite cohesive blend

To determine the optimal mixing time and reliable comparisons between the different scales, mixing kinetics have been

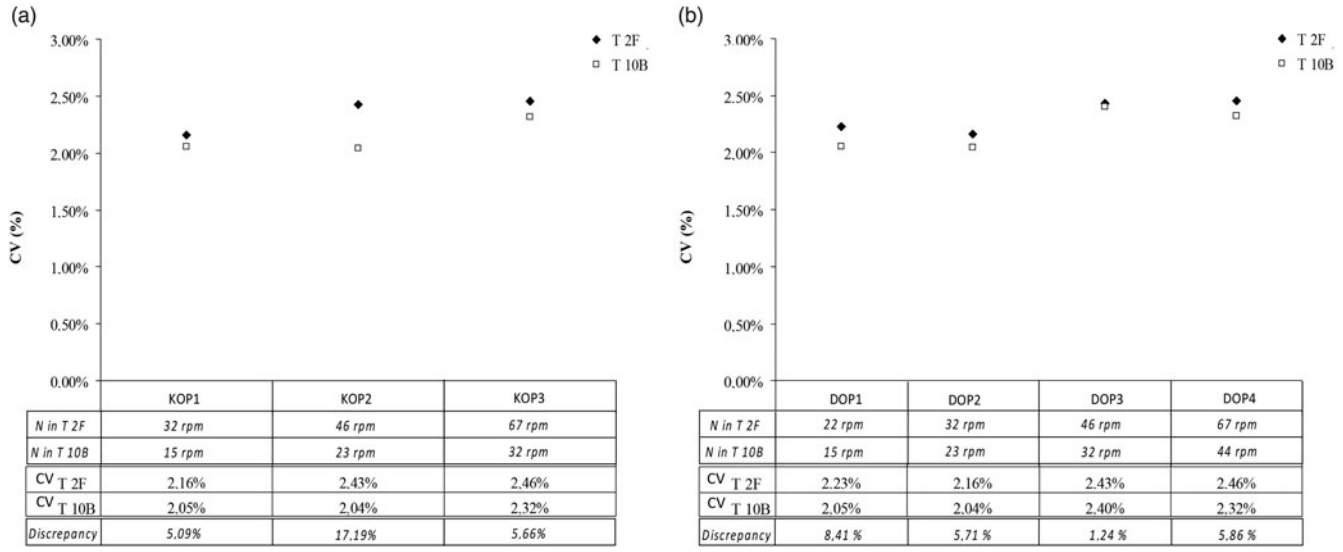

	KOP1	KOP2	KOP3
N in T 2F	32 rpm	46 rpm	67 rpm
N in T 10B	15 rpm	23 rpm	32 rpm
CV T 2F	2.16%	2.43%	2.46%
CV T 10B	2.05%	2.04%	2.32%
Discrepancy	5.09%	17.19%	5.66%

	DOP1	DOP2	DOP3	DOP4
N in T 2F	22 rpm	32 rpm	46 rpm	67 rpm
N in T 10B	15 rpm	23 rpm	32 rpm	44 rpm
CV T 2F	2.23%	2.16%	2.43%	2.46%
CV T 10B	2.05%	2.04%	2.40%	2.32%
Discrepancy	8.41 %	5.71 %	1.24 %	5.86 %

Figure 6. CV obtained for the different kinematic operating points KOP1, KOP2, and KOP3 (Figure 5(a)) and for the dynamic operating points DOP1, DOP2, DOP3, and DOP4 (Figure 5(b)) for the free flowing mixture after 500 revolutions.

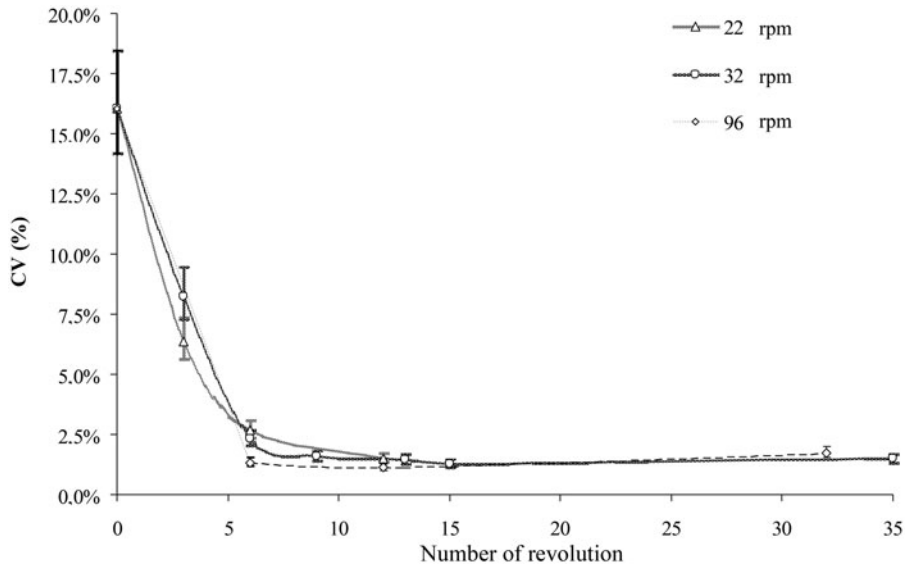

Figure 7. Mixing kinetics in Turbula® T2F for composite cohesive blend at 22, 32, and 96 rpm.

investigated in the Turbula® T2F (Figure 7) for the engine speeds 22, 32, and 96 rpm. The error bars in the figure correspond to the statistical errors due to the analysis based on 80 samples calculated with a χ^2 law for a 90% range of confidence. For these cohesive blends, the CV decreases very quickly, as a homogeneity close to the final one is reached after only 6 or 12 revolutions according to the engine speeds. These mixing kinetics also show that a greater engine speed leads more quickly to a greater homogeneity (i.e a lower CV). Indeed, the shear generated by a high engine speed probably leads to a disaggregating of the clusters of cohesive powder and favors mixing. CV has also been measured for a longer mixing time and show a slight decrease for the higher engine speed. As an example, the CV obtained with the engine speed of 96 rpm for 288 revolutions is equal to 1.01% against 1.91% for 32 revolutions.

Then, experiments performed in T2F, T10B, and T50A have been compared at the KOP1, KOP2, DOP1, and DOP1 for 6 and 12 revolutions (Figure 8). Since the values of CV are statistically assessed, the discrepancy between the CV obtained in the different scales is not relevant to compare results. We will consider in the following that two experiments are distinct, if there is no overlapping of the intervals of confidence (90%). It is the case, in particular, for the experiments involving a kinematic correspondence (left of Figures 8(a,b)).

The kinematic operating points lead to a different state of the mixture as in the case of the free-flowing blend. For the experiments realized in T2F and T10B, we observe a high overlapping of the error bars in case of dynamic correspondences at 6 and 12 revolutions. However, we can notice a significant difference for the values obtained in T50A. For 6 revolutions, the CV at the DOP2 is much higher in T50A than those obtained in T10B and T2F. The motion of the powder inside the mixer is related to the velocity/acceleration of the vessel. In the starting phases, which could be

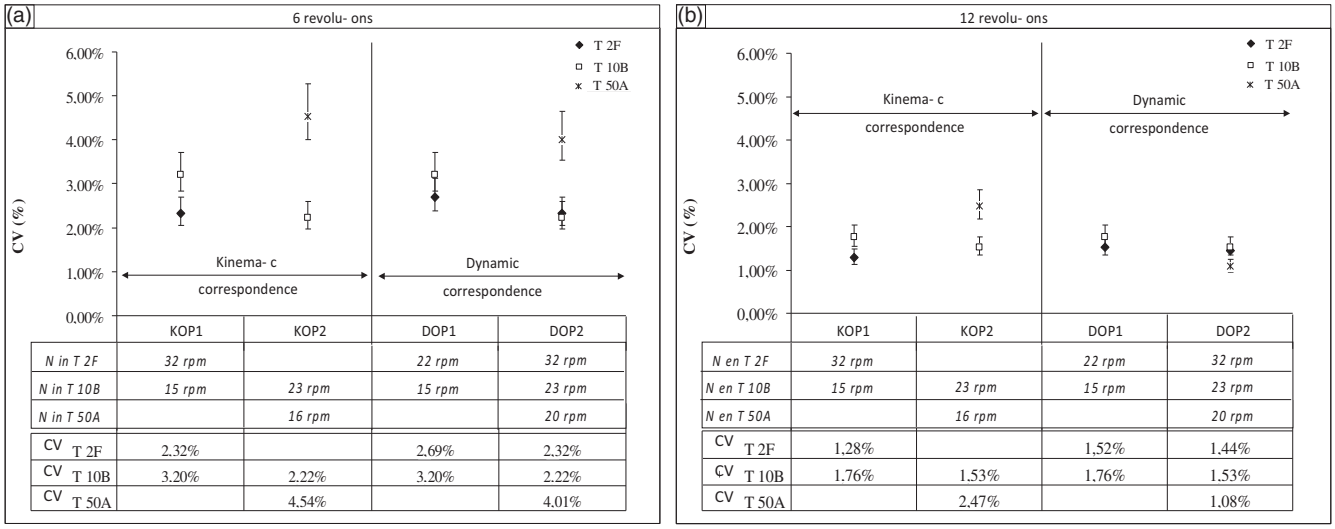

	KOP1	KOP2	DOP1	DOP2
N in T 2F	32 rpm		22 rpm	32 rpm
N in T 10B	15 rpm	23 rpm	15 rpm	23 rpm
N in T 50A		16 rpm		20 rpm
CV T 2F	2.32%		2,69%	2.32%
CV T 10B	3.20%	2.22%	3.20%	2.22%
CV T 50A		4.54%		4.01%

	KOP1	KOP2	DOP1	DOP2
N en T 2F	32 rpm		22 rpm	32 rpm
N en T 10B	15 rpm	23 rpm	15 rpm	23 rpm
N en T 50A		16 rpm		20 rpm
CV T 2F	1,28%		1,52%	1.44%
CV T 10B	1.76%	1.53%	1.76%	1.53%
CV T 50A		2,47%		1.08%

Figure 8. CV obtained for the operating points KOP1, KOP2, DOP1, and DOP2 at 6 (Figure 7(a)) and 12 (Figure 7(b)) revolutions for the composite cohesive blend.

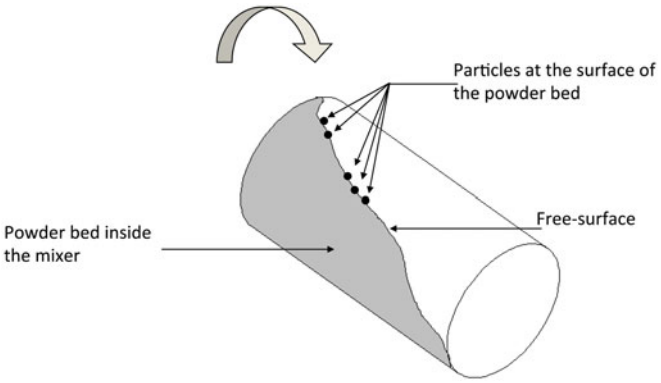

Figure 9. Diagram of the interior of the mixing vessel highlighting the position of the powder bed and the free surface where particles are moving.

more or less long according to the considered mixer sizes, the engine speed increases to reach the target value. As a result, the particles are submitted to different velocities or accelerations leading to different blend homogeneities. Due to the inertia related to the mass of the whole container plus that of the powder, it is likely that in the T50A, the acceleration is less significant than in smaller tanks, the starting phase is longer, in turn leading to a higher CV.

For 12 revolutions, the starting phase has ended and the flowing regime of the powder inside the mixer is established. In this case, the CV in the T50A for DOP2 is smaller than those obtained in T2F and T10B, as it was already observed for the FFB in the case of dynamic correspondence, suggesting that the efficiency of the mixer increases with its size. This tendency has been previously observed by (Cleary and Sinnott 2008) in V-blender. They found that in the case of a scale-up only based on the Froude number, the mixing quality is superior for the higher blender size. This phenomenon could be explained by increase of the free surface of the powder bed with the size of the mixer. Indeed, for a larger free surface, the falling and rolling distances for particles increase and lead to enhancement of the shear forces inside the mixer as illustrated in Figure 9. For cohesive powder like the composite blend, particles will probably dissociate more easily and the diffusion mechanisms, which favor intimate mixing (Lacey 1954), will be more efficient. Increasing the filling ratio with the mixer size could be a way to validate this hypothesis. Indeed an increase in the filling ratio will induce a decrease of the free surface.

The KOP and DOP have been defined on the basis of maximum velocity and maximum acceleration, respectively. In Figure 4, the maximum velocities are reached at 0.44 T and 0.94 T, which corresponds to horizontal translation motions of the blender (Mayer-Laigle, Gatumel, and Berthiaux 2015). In the same way, the maximum acceleration is reached for the first time in the period between 0.35 T and 0.45 T and between 0.85 T and 0.95 T for the second time when the vessel is reversed. In the previous part, we have shown that the dynamic criteria are more efficient to predict the quality of the mixture than the kinematic one. Thus, we can assume that the reverse phases are more efficient to achieve the mixture due to cascading of particles than translation phases where particles are embedded in the powder bed and have less space to move.

5. Conclusion

Geometric, kinematic, and dynamic similarities were studied, thanks to a Solidworks® simulation carried out for three sizes of the Turbula® blender. From these, kinematic and dynamic criteria for scaling-up those mixers were suggested on the basis of equal velocities or Froude numbers for a reference point at the bottom of the vessel. In parallel, flow regimes have been defined according to the different engine speeds. The mixture homogeneity, estimated from the coefficient of variation of samples' compositions, has been compared for different kinematic and dynamic operating points for an easy flowing blend and a cohesive blend. Whatever the blend considered, it seems that scaling-up on the basis of kinematic criteria does not allow reaching a similar mixture quality in each blender. The dynamic criterion leads to a better correlation between results obtained in T2F (lab scale) and T10B (pilot scale), most likely because the mixing and segregation mechanisms are similar in both sizes.

The scale-up at the industrial scale (T50A) has only been achieved for the composite cohesive blend and seems less obvious. Indeed, for short mixing time, the mixture quality obtained in a T50A is inferior to those obtained at pilot or lab scale. This may be explained by the larger inertia of the T50A which does not allow to reach immediately the set speed when starting agitation. In contrast, for a longer mixing time, the quality of the mixture is slightly higher in the largest mixers. Indeed the free surface area is markedly increased at this scale. It induces greater falling and rolling distances for particles leading to an increase of shear forces inside the mixer, favoring diffusion mechanism. A study of the influence of the filling ratio may validate this assumption and could be performed in further work. In addition, mixing of free-flowing powders like the free-flowing blend in the T50A should complete this work in order to clarify the effect of segregation mechanisms.

Abbreviations

CV	coefficient of variation
D50	median particle size
DI	dispersion index
DOP	dynamic operating point
Fr	Froude number
KOP	kinematic operating point
I_{carr}	Carr's index
N	Engine speed
R_H	Hausner's ratio
T	period of rotation of the tank
T2F, T10B, T50A	name of the different scales of Turbula® mixer
ρ_a	bulk density
ρ_p	packed density
μ :	mean of sample compositions
σ	standard deviation of sample compositions

Acknowledgment

We would like to thank Laurent Devriendt for his skillful help during the experimental work and Luc Penazzi for his technical support during the Solidworks® simulation.

Funding

The authors acknowledge the French agency for research, Agence Nationale de la Recherche (ANR), for its financial support through the MASCOTE project (ref ANR-08- MAPR-0002).

References

Alexander, A., T. Shinbrot, and F. J. Muzzio. 2002. Scaling surface velocities in rotating cylinders as a function of vessel radius, rotation rate, and particle size. *Powder Technology* 126 (2):174–90.

Ammarcha, C., C. Gatumel, J. L. Dirion, M. Cabassud, V. Mizonov, and H. Berthiaux. 2013. Transitory powder flow dynamics during emptying of a continuous mixer. *Chemical Engineering and Processing: Process Intensification* 65:68–75. doi: 10.1016/j.cep.2012.12.004.

Bridgwater, J. 2012. Mixing of powders and granular materials by mechanical means—A perspective. *Particuology* 10 (4):397–427. doi: 10.1016/j.partic.2012.06.002.

Carr, R. L. 1970. Particle behaviour storage and flow. *British Chemical Engineering* 15 (12):1541–1549.

Cavinato, M., R. Artoni, M. Bresciani, P. Canu, and A. C. Santomaso. 2013. Scale-up effects on flow patterns in the high shear mixing of cohesive powders. *Chemical Engineering Science* 102:1–9. doi: 10.1016/j.ces.2013.07.037.

Cleary, P. W., and M. D. Sinnott. 2008. Assessing mixing characteristics of particle-mixing and granulation devices. *Particuology* 6 (6):419–44. doi: 10.1016/j.partic.2008.07.014.

Demeyre, J. F. 2007. Caractérisation de l'homogénéité de mélange de poudres et de l'agitateur en mélange triaxe. PhD. thesis, Université de Toulouse.

Ding, Y. L., R. N. Forster, J. P. K. Seville, and D. J. Parker. 2001. Scaling relationships for rotating drums. *Chemical Engineering Science* 56 (12):3737–50. doi: 10.1016/S0009-2509(01)00092-6.

Hausner, H. H. 1967. Friction condition in a mass of metal powder. *International Journal of Powder Metallurgy* 3:7–13.

Henein, H., J. K. Brimacombe, and A. P. Watkinson. 1983. The modeling of transverse solids motion in rotary kilns. *Metallurgical Transactions B* 14 (2):207–20. doi: 10.1007/BF02661017.

James, J., M. Cooke, L. Trinh, R. Hou, P. Martin, A. Kowalski, and T. L. Rodgers. 2017. Scale-up of batch rotor–stator mixers. Part 1—power constants. *Chemical Engineering Research and Design* 124:313–20. doi: 10.1016/j.cherd.2017.06.020.

Kushner, J. 2012. Incorporating Turbula mixers into a blending scale-up model for evaluating the effect of magnesium stearate on tablet tensile strength and bulk specific volume. *International Journal of Pharmaceutics* 429 (1–2):1–11. doi: 10.1016/j.ijpharm.2012.02.040.

Lacey, P. M. C. 1954. Developments in the theory of particle mixing. *Journal of Applied Chemistry* 4 (5):257–68. doi: 10.1002/jctb.5010040504.

Landin, M., P. York, M. J. Cliff, R. C. Rowe, and A. J. Wigmore. 1996. Scale-up of a pharmaceutical granulation in fixed bowl mixer-granulators. *International Journal of Pharmaceutics* 133 (1–2):127–31. doi: 10.1016/0378-5173(95)04427-2.

Langhaar, H. L. 1980. *Dimensional analysis and theory of models*. Huntington, New York: John Wiley & Sons.

Marmur, B. L., and T. J. Heindel. 2017. Scale effects on double-screw granular mixing. *Powder Technology* 321:74–88. doi: 10.1016/j.powtec.2017.07.067.

Massol-Chaudeur, S., H. Berthiaux, and J. A. Dodds. 2002. Experimental study of the mixing kinetics of binary pharmaceutical powder mixture in a laboratory hoop mixe. *Chemical Engineering Science* 57(19):4053–65. doi: 10.1016/S0009-2509(02)00262-2.

Mayer-Laigle, C., C. Gatumel, and H. Berthiaux. 2015. Mixing dynamics for easy flowing powders in a lab scale Turbula® mixer. *Chemical Engineering Research and Design* 95:248–61. doi: 10.1016/j.cherd.2014.11.003.

Mellmann, J. 2001. The transverse motion of solids in rotating cylinders—forms of motion and transition behavior. *Powder Technology* 118 (3):251–70. doi: 10.1016/S0032-5910(00)00402-2.

Midoux, N. 1985. Mécanique et rhéologie des fluides en génie chimique. *Technique et Documentation. Lavoisier* 149–152.

Nakamura, H., Y. Miyazaki, Y. Sato, T. Iwasaki, and S. Watano. 2009. Numerical analysis of similarities of particle behavior in high shear mixer granulators with different vessel sizes. *Advanced Powder Technology* 20 (5):493–501. doi: 10.1016/j.apt.2009.05.006.

Qi, F., T. J. Heindel, and M. M. Wright. 2017. Numerical study of particle mixing in a lab-scale screw mixer using the discrete element method. *Powder Technology* 308:334–45. doi: 10.1016/j.powtec.2016.12.043.

Redaelli, I., F. Ceccato, C. di Prisco, and P. Simonini. 2017. Solid-fluid transition in granular flows: MPM simulations with a new constitutive approach. *Procedia Engineering* 175:80–5. doi: 10.1016/j.proeng.2017.01.028.

Savage, S. B. 1984. The mechanics of rapid granular flows. *Advances in applied mechanics* 24:289–366.

Shah, U. V., V. Karde, C. Ghoroi, and J. Y. Y. Heng. 2017. Influence of particle properties on powder bulk behaviour and processability. *International Journal of Pharmaceutics* 518 (1–2):138–54. doi: 10.1016/j.ijpharm.2016.12.045.

Shenoy, P., F. Innings, K. Tammel, J. Fitzpatrick, and L. Ahrné. 2015. Evaluation of a digital colour imaging system for assessing the mixture quality of spice powder mixes by comparison with a salt conductivity method. *Powder Technology* 286:48–54. doi: 10.1016/j.powtec.2015.07.034.

Suzuki, Y., T. Kato, Y. Kikkawa, T. Suzuki, N. Wakiyama, and K. Terada. 2015. Scale-up and blender change model for the pharmaceutical lubricated mixing process. *Powder Technology* 280:113–8. doi: 10.1016/j.powtec.2015.04.052.

Wohlhart, K. 1981. A dynamic analysis of the Turbula, International Symposium on Gearing and Power Transmissions, Tokyo, 425–430.

Xiao, X.,. Y. Tan, H. Zhang, R. Deng, and S. Jiang. 2017. Experimental and DEM studies on the particle mixing performance in rotating drums: Effect of area ratio. *Powder Technology* 314:182–63. doi: 10.1016/j.powtec.2017.01.044.

Yamamoto, M., S. Ishihara, and J. Kano. 2016. Evaluation of particle density effect for mixing behavior in a rotating drum mixer by DEM simulation. *Advanced Powder Technology* 27 (3):864–70. doi: 10.1016/j.apt.2015.12.013.

Yang, R. Y., A. B. Yu, L. McElroy, and J. Bao. 2008. Numerical simulation of particle dynamics in different flow regimes in a rotating drum. *Powder Technology* 188 (2):170–7. doi: 10.1016/j.powtec.2008.04.081.

Yijie, G., F. J. Muzzio, and M. G. Ierapetritou. 2013. Scale-up strategy for continuous powder blending process. *Powder Technology* 235: 55–69.

Zhou, Q., and D. A. V. Morton. 2012. Drug–lactose binding aspects in adhesive mixtures: Controlling performance in dry powder inhaler formulations by altering lactose carrier surfaces. *Advanced Drug Delivery Reviews* 64 (3):275–84. doi: 10.1016/j.addr.2011.07.002.